

CONVERGENCE OF LONG-TIME STABLE VARIABLE-STEP ARBITRARY ORDER ETD-MS SCHEME FOR GRADIENT FLOWS WITH LIPSCHITZ NONLINEARITY

WENBIN CHEN, ZHAOHUI FU, SHUFEN WANG, AND XIAOMING WANG

ABSTRACT. We analyze a variable-step extension of a family of arbitrarily high-order exponential time differencing multistep (ETD-MS) schemes recently developed by the authors. We prove that the schemes are unconditionally stable in the sense that a modified energy—representing a slight perturbation of the original energy—decreases monotonically over time, provided the nonlinearity is Lipschitz continuous in some appropriate sense. Moreover, we establish optimal-order convergence under mild conditions on the time-step size and local time-step ratio. Numerical experiments on the thin film epitaxial growth model without slope selection, employing a novel variable-step second-order scheme, validate the theoretical findings as well as its potential in developing highly efficient time-adaptive solution.

1. INTRODUCTION

The long-time behavior of many mathematical models is of great interest, particularly in the context of gradient flows arising in materials science, where physically important processes such as coarsening evolve over extended time scales. Capturing such dynamics efficiently poses significant computational challenges, thereby motivating the development of highly effective numerical methods.

Two key strategies are commonly employed to enhance computational efficiency: 1. High-order schemes, which enable the use of relatively large time steps while maintaining a prescribed accuracy, thus reducing the total number of steps required to reach a given final time. 2. Adaptive (variable) time-stepping, which allows time steps to be dynamically adjusted, taking larger steps when the system evolves slowly, and smaller steps when rapid changes occur.

A substantial body of literature exists on designing energy-stable schemes and conducting long-time simulations of various gradient flows in materials science and fluid dynamics. Notable approaches include convex splitting, truncation techniques, the scalar auxiliary variable (SAV) method, and the invariant energy quadratization (IEQ) method; see, for example, [22, 23, 25, 41–45, 48] and references therein.

Exponential time differencing (ETD) is a particularly attractive class of time discretization techniques that achieves high-order accuracy through the exact treatment of the linear

2020 *Mathematics Subject Classification.* 65M12, 65M70, 65Z05.

Key words and phrases. Exponential time differencing, long time energy stability, arbitrary order scheme, multi-step method, variable-step method, convergence, gradient flow, epitaxial thin film growth.

part and the application of Duhamel's principle to the nonlinear part [13, 19, 20]. The resulting formulation introduces a nonlinear integral term, for which two primary approximation strategies are commonly adopted: Runge–Kutta (RK) methods [17, 28, 29] and multistep (MS) methods [27, 29, 30]. These approximations are typically explicit in nature to preserve the computational efficiency of the ETD framework.

While it is relatively straightforward to formally construct variable step arbitrarily high-order ETD schemes via the RK or MS approaches, ensuring energy stability is far more delicate, primarily due to the explicit treatment of the nonlinear term. Among these approaches, the ETD-RK method has been extensively studied and applied, offering a flexible framework to achieve high-order accuracy, see [7, 8, 40, 63–65]. Recent advances also have addressed this issue by incorporating stabilization techniques into the ETD-MS framework, leading to energy-stable schemes of second order [4, 31], third order [5, 16], and arbitrary order [6], all under the assumption of a constant time step.

The primary objective of this paper is to extend the energy-stable ETD-MS framework to the variable time-step setting for a class of nonlinear gradient flows, building on our recent work in [6]. We prove that the proposed variable-step ETD-MS schemes remain energy stable in the sense that a modified energy—a slight perturbation of the original energy—decreases monotonically over time. In addition, we establish that the schemes achieve optimal convergence rates under mild conditions on the time-step size and local time-step ratio.

Unless specified otherwise, we denote C a generic constant which may depend on ϵ , the exact solution u , the initial value u_0 , and the final time T , but is independent of time step-size τ . The standard Sobolev space notations follow from [1].

The rest of the paper is organized as follows. The continuous problem is introduced in section 2. We introduce the variable-step arbitrary high-order ETD-MS based scheme and verify its energy stability in section 3. The convergence with optimal rate under a mild assumption on the step-size and the ratio of different step-sizes is established in section 4. The applicability to the no-slope selection (NSS) thin-film epitaxial growth model is explained in section 5. Numerical experiments on the no-slope selection thin film epitaxial growth model that are consistent with our theory are reported in section 6. Conclusion remarks are provided in section 7.

2. THE CONTINUOUS PROBLEM

Let $X \hookrightarrow \mathcal{H} \hookrightarrow X'$ be a standard triple of Hilbert spaces. And let \mathcal{L} be a positive definite linear operator on \mathcal{H} which maps X to X' , the dual space of X . Denoting $\mathcal{L}^{1/2}$ the square root of \mathcal{L} . Let $E(u)$ be an energy functional on a Hilbert space \mathcal{H} (with the domain being a subspace of \mathcal{H}) given by

$$E(u) = \frac{\epsilon}{2} \|\mathcal{L}^{1/2} u\|_{\mathcal{H}}^2 + \mathcal{F}(u).$$

The associated gradient flow with mobility M can then be formulated as follows

$$(2.1) \quad \frac{\partial u}{\partial t} = -M \frac{\delta E}{\delta u}.$$

where $\frac{\delta E}{\delta u}$ denotes the variational derivative of E .

Denoting the variational derivative of \mathcal{F} as $-F$, i.e., $\frac{\delta \mathcal{F}}{\delta u} = -F$, we deduce that the associated gradient flow takes the form of

$$(2.2) \quad \frac{\partial u(t)}{\partial t} + \epsilon \mathcal{L}u(t) = F(u(t)).$$

when $M = 1$.

Taking the inner product of (2.1) with $\frac{\delta E}{\delta u}$ in \mathcal{H} leads to the energy equality:

$$(2.3) \quad \frac{dE(u)}{dt} = -M \left\| \frac{\delta E}{\delta u} \right\|_{\mathcal{H}}^2.$$

We will impose the following three assumptions on (2.2), with assumption 1 – 2 for energy stability and the third one for convergence analysis:

- (1) The operator \mathcal{L} is self-adjoint nonnegative on \mathcal{H} .

Thus we can define operators $\mathcal{L}^{\alpha/2}$ for any $\alpha \geq 0$. The domain of operator $\mathcal{L}^{\alpha/2}$ is denoted by V^α with the norm on V^α given by $\|v\|_{V^\alpha} = \|\mathcal{L}^{\alpha/2}v\|_{\mathcal{H}}$. For $\alpha = 1$ and $\alpha = 0$, it is abbreviated as $\mathcal{D}(\mathcal{L}^{\frac{1}{2}}) = V$ and $\mathcal{D}(\mathcal{L}^0) = \mathcal{H}$, respectively.

- (2) The nonlinear term is Lipschitz continuous in the sense that: $\exists \beta \geq 0, \gamma \geq 0$, and $C_L > 0$ with $\beta + \gamma \leq 1$, such that

$$(2.4) \quad \|F(u) - F(v)\|_{V^{-\beta}} \leq C_L \|u - v\|_{V^\gamma},$$

where $V^{-\beta}$ is the dual space to V^β induced by the inner product on \mathcal{H} .

- (3) $F(u(\cdot, t))$ has the boundedness property in the sense that for any $T > 0$, $\exists C = C(T) > 0$, s.t.

$$(2.5) \quad \|F(u)\|_{H^k(0, T; V^{-\beta})} \leq C.$$

Remark 2.1. *The restriction of $\beta + \gamma \leq 1$ in the second assumption is for convergence only.*

Remark 2.2. *Likewise, assumption 3 is used in the error estimate only. It can be verified for many systems such as the no-slope selection thin film epitaxial growth model investigated in the numerical experiment in this paper provided that the initial data is sufficiently smooth.*

3. THE TEMPORAL SEMI-DISCRETE SCHEME AND ITS LONG TIME STABILITY

The main purpose of this section is to introduce the variable step high-order ETD-MS based time discretization of the gradient flow (2.2), and prove the long time energy stability of the scheme. The scheme is a variable-step version of the arbitrary high-order ETD-MS scheme that was introduced in [6]. The long time stability is in the sense that there is a modified energy that decreases in time. The modified energy is a small perturbation of the original one.

3.1. The scheme. To solve (2.2) numerically, we propose the following ETD-MS based variable-step temporal semi-discrete numerical scheme: find $u^{n+1}(t)$ such that

$$(3.1) \quad \frac{du^{n+1}(t)}{dt} + \epsilon \mathcal{L}u^{n+1}(t) + A\tau^k \frac{d}{dt} \mathcal{L}^{p(k)}u^{n+1}(t) = \sum_{i=0}^{k-1} \ell_i(t - t_n) F(u^{n-i}), \quad t \in [t_n, t_{n+1}],$$

with $u^{n+1}(t) = u^n(t)$ for $t \in [0, t_n]$. The temporal step-sizes are denoted by $\tau_n := t_{n+1} - t_n$, and $\tau = \max \tau_j$. Moreover, we denote u^{n-i} the numerical solution at time t_{n-i} and $\ell_i(s)$ the shifted (to the negative range) Lagrange basis polynomial of degree k with the form of

$$(3.2) \quad \ell_i(s) = \prod_{\substack{0 \leq m \leq k-1 \\ m \neq i}} \frac{\sum_{j=1}^m \tau_{n-j} + s}{\sum_{j=1}^m \tau_{n-j} - \sum_{j=1}^i \tau_{n-j}} = \prod_{\substack{0 \leq m \leq k-1 \\ m \neq i}} \frac{\sum_{j=1}^m \frac{\tau_{n-j}}{\tau} + \frac{s}{\tau}}{\sum_{j=1}^m \frac{\tau_{n-j}}{\tau} - \sum_{j=1}^i \frac{\tau_{n-j}}{\tau}} = \sum_{j=0}^{k-1} \xi_{i,j} s^j,$$

where $\{\xi_{i,j}\}_{j=0}^{k-1}$ are coefficients of the polynomial $\ell_i(s)$. Note that $\frac{\tau_j}{\tau} \leq 1$ for any $j \leq n$, it is not hard to see $\xi_{i,j} \sim \mathcal{O}(\tau^{-j})$.¹

The scheme is the variable-step version of the scheme proposed recently by the authors [6]. As in that work, we have employed a Dupont-Douglas type regularization term $A\tau^k \frac{d}{dt} \mathcal{L}^{p(k)}u^{n+1}(t)$ in order to enhance stability. The parameters $A, p(k)$, associated with the strength of regularization, will be specified later.

3.2. Energy stability. In this subsection, we establish the energy stability for the scheme (3.1). The proof is similar to the stability proof in the constant step-size case presented in [6] adapted to the current variable-step scenario. The interpolation inequalities utilized below involving various exponents of V , i.e., the domain of various powers of \mathcal{L} , follow from the spectral representation of the self-adjoint non-negative operator \mathcal{L} [34] and Hölder's inequality.

First we present a few interpolation estimates that will be used later.

Lemma 3.1. *Let β, γ be two non-negative numbers, $q \in [0, 1]$, and $p(k)$ is chosen so that $p(k) > \max\{\beta, \gamma\}$. Then for any $u \in V^\beta$ and $v \in V^\gamma$, and arbitrary positive constants \hat{C}, \tilde{C} , the following inequalities hold for different cases of β and γ .*

(1) *If $\min\{\beta, \gamma\} > 0$, we have*

$$(3.3) \quad \tau \|u\|_{V^\beta} \|v\|_{V^\gamma} \leq C_1 \|u\|_{\mathcal{H}}^2 + C_2 \tau^{\frac{2qp(k)}{\beta}} \|u\|_{V^{p(k)}}^2 + C_3 \|v\|_{\mathcal{H}}^2 + C_4 \tau^{\frac{2(1-q)p(k)}{\gamma}} \|v\|_{V^{p(k)}}^2,$$

¹We have suppressed the dependence of ℓ_i on n for simplicity. The bound on ℓ_i is uniform in n provided that the ratio between the maximum time-step and the minimum time-step in the neighboring k steps is bounded by a constant independent of the step-sizes.

where

$$(3.4) \quad \begin{aligned} C_1(\hat{C}) &= \frac{1 - \beta/p(k)}{2} \hat{C}^{1/(1-\beta/p(k))}, & C_2(\hat{C}) &= \frac{\beta}{2p(k)} \hat{C}^{-p(k)/\beta}, \\ C_3(\tilde{C}) &= \frac{1 - \gamma/p(k)}{2} \tilde{C}^{1/(1-\gamma/p(k))}, & C_4(\tilde{C}) &= \frac{\gamma}{2p(k)} \tilde{C}^{-p(k)/\gamma}. \end{aligned}$$

(2) If $\min\{\beta, \gamma\} = 0$ but $\max\{\beta, \gamma\} > 0$, we have

$$(3.5) \quad \tau \|u\|_{V^\beta} \|v\|_{V^\gamma} \leq \frac{1}{2} \|u\|_{\mathcal{H}}^2 + C_3 \|v\|_{\mathcal{H}}^2 + C_4 \tau^{\frac{2p(k)}{\gamma}} \|v\|_{V^{p(k)}}^2, \quad \text{if } \beta = 0, \gamma > 0$$

$$(3.6) \quad \tau \|u\|_{V^\beta} \|v\|_{V^\gamma} \leq C_1 \|u\|_{\mathcal{H}}^2 + C_2 \tau^{\frac{2p(k)}{\beta}} \|u\|_{V^{p(k)}}^2 + \frac{1}{2} \|v\|_{\mathcal{H}}^2, \quad \text{if } \beta > 0, \gamma = 0.$$

(3) If $\max\{\beta, \gamma\} = 0$, we have

$$(3.7) \quad \tau \|u\|_{V^\beta} \|v\|_{V^\gamma} \leq \frac{\tau}{2} \|u\|_{\mathcal{H}}^2 + \frac{\tau}{2} \|v\|_{\mathcal{H}}^2.$$

Proof. For $\beta, \gamma > 0$, we employ interpolation inequality to control $\|\cdot\|_{V^\beta}$, $\|\cdot\|_{V^\gamma}$ by $\|\cdot\|_H$ and $\|\cdot\|_{V^{p(k)}}$, and we have:

$$(3.8) \quad \tau \|u\|_{V^\beta} \|v\|_{V^\gamma} \leq \tau \|u\|_{\mathcal{H}}^{1-\beta/p(k)} \|u\|_{V^{p(k)}}^{\beta/p(k)} \cdot \|v\|_{\mathcal{H}}^{1-\gamma/p(k)} \|v\|_{V^{p(k)}}^{\gamma/p(k)}.$$

Denoting the right hand side (RHS) of (3.8) by I_1 , and invoking Young's inequality twice, we deduce

$$(3.9) \quad \begin{aligned} I_1 &\leq \frac{1}{2} \tau^{2q} \|u\|_{\mathcal{H}}^{2-2\beta/p(k)} \|u\|_{V^{p(k)}}^{2\beta/p(k)} + \frac{1}{2} \tau^{2-2q} \|v\|_{\mathcal{H}}^{2-2\gamma/p(k)} \|v\|_{V^{p(k)}}^{2\gamma/p(k)} \\ &\leq \frac{1 - \beta/p(k)}{2} \left(\hat{C} \|u\|_{\mathcal{H}}^{2-2\beta/p(k)} \right)^{1/(1-\beta/p(k))} + \frac{\beta}{2p(k)} \left(\frac{\tau^{2q}}{\hat{C}} \|u\|_{V^{p(k)}}^{2\beta/p(k)} \right)^{p(k)/\beta} \\ &\quad + \frac{1 - \gamma/p(k)}{2} \left(\tilde{C} \|v\|_{\mathcal{H}}^{2-2\gamma/p(k)} \right)^{1/(1-\gamma/p(k))} + \frac{\gamma}{2p(k)} \left(\frac{\tau^{2-2q}}{\tilde{C}} \|v\|_{V^{p(k)}}^{2\gamma/p(k)} \right)^{p(k)/\gamma} \\ &= C_1 \|u\|_{\mathcal{H}}^2 + C_2 \tau^{\frac{2qp(k)}{\beta}} \|u\|_{V^{p(k)}}^2 + C_3 \|v\|_{\mathcal{H}}^2 + C_4 \tau^{\frac{2(1-q)p(k)}{\gamma}} \|v\|_{V^{p(k)}}^2. \end{aligned}$$

The proof for the case of either or both β and γ are zero is similar. This completes the proof of Lemma 3.1. \square

Remark 3.2. Note that the estimates (3.5)–(3.7) are limit cases of (3.3) with the constants \hat{C} and \tilde{C} chosen appropriately.

Now we prove the energy stability. For simplicity, we denote $\|\cdot\|_{L^2(t_i, t_j; V^\alpha)}$ by $\|\cdot\|_{L^2(I_i^{j-i}; V^\alpha)}$ hereafter.

Lemma 3.3. *For scheme (3.1), one has the following energy estimate.*

$$\begin{aligned}
 & E(u^{n+1}) - E(u^n) + \left\| \frac{du^{n+1}(t)}{dt} \right\|_{L^2(I_n^1; \mathcal{H})}^2 + A\tau^k \left\| \frac{du^{n+1}(t)}{dt} \right\|_{L^2(I_n^1; V^{p(k)})}^2 \\
 (3.10) \quad & \leq \sum_{j=0}^{k-1} C_L \tau_{n-j}^{\frac{1}{2}} \left\| 1 - \sum_{i=-1}^{j-1} \ell_i(t - t_n) \right\|_{L^2(I_n^1)} \left\| \frac{du^{n-j+1}(t)}{dt} \right\|_{L^2(I_{n-j}^1; V^\gamma)} \left\| \frac{du^{n+1}(t)}{dt} \right\|_{L^2(I_n^1; V^\beta)},
 \end{aligned}$$

where the convention $\ell_{-1}(t - t_n) = 0$ has been used.

Proof. To establish the desired energy estimates, we subtract $F(u^{n+1}(t))$ from both sides of (3.1) and take the inner product of the result with $\frac{du^{n+1}(t)}{dt}$ on \mathcal{H} , which gives

$$\begin{aligned}
 & \left\| \frac{du^{n+1}(t)}{dt} \right\|_{\mathcal{H}}^2 + A\tau^k \left\| \frac{du^{n+1}(t)}{dt} \right\|_{V^{p(k)}}^2 + \frac{d}{dt} E(u^{n+1}(t)) \\
 (3.11) \quad & = \left(\sum_{i=0}^{k-1} \ell_i(t - t_n) F(u^{n-i}) - F(u^{n+1}(t)), \frac{du^{n+1}(t)}{dt} \right)_{\mathcal{H}}.
 \end{aligned}$$

Integrating from t_n to t_{n+1} gives

$$\begin{aligned}
 & \left\| \frac{du^{n+1}(t)}{dt} \right\|_{L^2(I_n^1; \mathcal{H})}^2 + A\tau^k \left\| \frac{du^{n+1}(t)}{dt} \right\|_{L^2(I_n^1; V^{p(k)})}^2 + E(u^{n+1}) - E(u^n) \\
 (3.12) \quad & = \int_{t_n}^{t_{n+1}} \left(\sum_{i=0}^{k-1} \ell_i(t - t_n) F(u^{n-i}) - F(u^{n+1}(t)), \frac{du^{n+1}(t)}{dt} \right)_{\mathcal{H}} dt.
 \end{aligned}$$

Note that the sum of the Lagrange basis functions equals one, i.e., $\sum_{i=0}^{k-1} \ell_i(t - t_n) \equiv 1$. Thus terms within the integral in RHS of (3.11) (denoted by NLT) can be rewritten as

$$\begin{aligned}
\text{NLT} &= \left(\sum_{i=0}^{k-1} \ell_i(t - t_n) (F(u^{n-i}) - F(u^{n+1}(t))), \frac{du^{n+1}(t)}{dt} \right)_{\mathcal{H}} \\
&= \left(\sum_{i=0}^{k-1} \ell_i(t - t_n) (F(u^{n-i}) - F(u^{n-i+1}) + \dots + F(u^n) - F(u^{n+1}(t))), \frac{du^{n+1}(t)}{dt} \right)_{\mathcal{H}} \\
&= \left(\sum_{i=0}^{k-1} \ell_i(t - t_n) (F(u^n) - F(u^{n+1}(t))), \frac{du^{n+1}(t)}{dt} \right)_{\mathcal{H}} \\
&\quad + \sum_{j=1}^{k-1} \left(\sum_{i=j}^{k-1} \ell_i(t - t_n) (F(u^{n-j}) - F(u^{n-j+1})), \frac{du^{n+1}(t)}{dt} \right)_{\mathcal{H}} \\
&= \left(F(u^n) - F(u^{n+1}(t)), \frac{du^{n+1}(t)}{dt} \right)_{\mathcal{H}} \\
(3.13) \quad &+ \sum_{j=1}^{k-1} \left(\left(1 - \sum_{i=0}^{j-1} \ell_i(t - t_n) \right) (F(u^{n-j}) - F(u^{n-j+1})), \frac{du^{n+1}(t)}{dt} \right)_{\mathcal{H}}.
\end{aligned}$$

Utilizing the Cauchy-Schwarz inequality and the Lipschitz continuity assumption (2.4), we deduce

$$\begin{aligned}
&\int_{t_n}^{t_{n+1}} \left(F(u^n) - F(u^{n+1}(t)), \frac{du^{n+1}(t)}{dt} \right)_{\mathcal{H}} dt \\
&\leq C_L \int_{t_n}^{t_{n+1}} \|u^n - u^{n+1}(t)\|_{V^\gamma} \left\| \frac{du^{n+1}(t)}{dt} \right\|_{V^\beta} dt \\
&\leq C_L \int_{t_n}^{t_{n+1}} \tau_n^{\frac{1}{2}} \left\| \frac{du^{n+1}(t)}{dt} \right\|_{L^2(I_n^1; V^\gamma)} \left\| \frac{du^{n+1}(t)}{dt} \right\|_{V^\beta} dt \\
&\leq C_L \tau_n \left\| \frac{du^{n+1}(t)}{dt} \right\|_{L^2(I_n^1; V^\gamma)} \left\| \frac{du^{n+1}(t)}{dt} \right\|_{L^2(I_n^1; V^\beta)} \\
(3.14) \quad &:= \text{NLT}_0,
\end{aligned}$$

where the last inequality follows from Hölder's inequality.

Similarly, the remaining terms in RHS of (3.12) can be estimated as

$$\begin{aligned}
 & \int_{t_n}^{t_{n+1}} \left(\left(1 - \sum_{i=0}^{j-1} \ell_i(t - t_n) \right) (F(u^{n-j}) - F(u^{n-j+1})) , \frac{du^{n+1}(t)}{dt} \right)_{\mathcal{H}} dt \\
 & \leq C_L \tau_{n-j}^{\frac{1}{2}} \left\| \frac{du^{n-j+1}(t)}{dt} \right\|_{L^2(I_{n-j}^1; V^\gamma)} \left\| \frac{du^{n+1}(t)}{dt} \right\|_{L^2(I_n^1; V^\beta)} \left\| 1 - \sum_{i=0}^{j-1} \ell_i(t - t_n) \right\|_{L^2(I_n^1)} \\
 (3.15) \quad & := \text{NLT}_j, \quad 1 \leq j \leq k-1.
 \end{aligned}$$

This completes the proof. \square

Next we give an upper bound on $\left\| 1 - \sum_{i=0}^{j-1} \ell_i(t - t_n) \right\|_{L^2(I_n^1)}$ and further provide the energy stability for our scheme (3.1). Recall that in (3.2), the Lagrange basis $\ell_i(s)$ is expressed as the polynomial of s with coefficients $\xi_{i,j}$. According to the properties of $\xi_{i,j}$, it's easy to see

$$\begin{aligned}
 (3.16) \quad & \left\| 1 - \sum_{i=0}^{j-1} \ell_i(t - t_n) \right\|_{L^2(I_n^1)} = \left\| 1 - \sum_{i=0}^{j-1} \sum_{r=0}^{k-1} \xi_{i,r}(t - t_n)^r \right\|_{L^2(I_n^1)} \leq C_j^* \tau^{1/2}, \quad 1 \leq j \leq k-1,
 \end{aligned}$$

where the constants C_j^* are independent of time step-size τ_i ($i \leq n$), τ and current time t .

For convenience, we follow the convention of $C_0^* = 1$ hereafter, and we introduce another sequence of positive constants \overline{C}_j through

$$(3.17) \quad \overline{C}_j := \sum_{r=0}^{k-1-j} C_{k-1-r}^* = \sum_{l=j}^{k-1} C_l^*.$$

It follows that

$$(3.18) \quad \overline{C}_j = \overline{C}_{j+1} + C_j^*, \quad \overline{C}_{k-1} = C_{k-1}^*.$$

We now introduce the following **modified energy**

$$(3.19) \quad \tilde{E}(u^n) = E(u^n) + C_L C_3 \sum_{j=1}^{k-1} \overline{C}_j \left\| \frac{du^{n-j+1}(t)}{dt} \right\|_{L^2(I_{n-j}^1; \mathcal{H})}^2 + C_L C_4 \sum_{j=1}^{k-1} \overline{C}_j \tau^k \left\| \frac{du^{n-j+1}(t)}{dt} \right\|_{L^2(I_{n-j}^1; V^{p(k)})}^2,$$

where both C_3 , C_4 depend on \hat{C} , \tilde{C} as specified in (3.4).

Remark 3.4. *It is easy to see that the second term on the right hand side is of the order of τ while the third term is of the order of τ^2 . Therefore, the modified energy is a small perturbation of the original energy E when the maximum time-step τ is small.*

Thanks to (3.4), C_1, C_3 can be made as small as we need so long as we set \hat{C}, \tilde{C} small enough. Therefore, for proper constants \hat{C}, \tilde{C} , and A , to be specified below, the following inequalities hold

$$(3.20) \quad 1 - C_L (C_3 + C_1 \bar{\mathcal{C}}_0) \geq C_L C_3 \bar{\mathcal{C}}_1,$$

$$(3.21) \quad A - C_L (C_4 + C_2 \bar{\mathcal{C}}_0) \geq C_L C_4 \bar{\mathcal{C}}_1.$$

Note that $C_0^* = 1$, and hence $\bar{\mathcal{C}}_0 = \bar{\mathcal{C}}_1 + 1$ according to (3.18). Therefore (3.20)–(3.21) are equivalent to

$$1 \geq C_L (C_3 + C_1) \bar{\mathcal{C}}_0,$$

$$A \geq C_L (C_4 + C_2) \bar{\mathcal{C}}_0.$$

This can be accomplished if we set \hat{C} and \tilde{C} small enough so that

$$(3.22) \quad (1 - \beta/p(k)) \hat{C}^{1/(1-\beta/p(k))} + (1 - \gamma/p(k)) \tilde{C}^{1/(1-\gamma/p(k))} \leq 2/(C_L \bar{\mathcal{C}}_0),$$

and then let

$$(3.23) \quad A = C_L \left(\frac{\beta}{2p(k)} \hat{C}^{-p(k)/\beta} + \frac{\gamma}{2p(k)} \tilde{C}^{-p(k)/\gamma} \right) \bar{\mathcal{C}}_0.$$

We have (3.20)–(3.21) with the choice of \hat{C}, \tilde{C} , and A .

We are now ready to prove the main result of the energy stability.

Theorem 3.5. *Let \hat{C} and \tilde{C} be chosen so that (3.22) is satisfied, and the stabilized coefficient A be specified in (3.23). Then the numerical scheme (3.1) is energy stable in the sense that*

$$(3.24) \quad \tilde{E}(u^{n+1}) \leq \tilde{E}(u^n), \quad \forall n \geq k.$$

Proof. By (3.16), the estimate (3.15) for NLT_j , $1 \leq j \leq k-1$ can be simplified to

$$(3.25) \quad \text{NLT}_j = C_L C_j^* \tau_n^{\frac{1}{2}} \tau_{n-j}^{\frac{1}{2}} \left\| \frac{du^{n-j+1}(t)}{dt} \right\|_{L^2(I_{n-j}^1; V^\gamma)} \left\| \frac{du^{n+1}(t)}{dt} \right\|_{L^2(I_n^1; V^\beta)}.$$

Applying Lemma 3.1 to (3.14) and (3.25), these nonlinear terms can be bounded further:

$$(3.26) \quad \begin{aligned} \text{NLT}_0 &\leq C_L \left[C_1 \left\| \frac{du^{n+1}(t)}{dt} \right\|_{L^2(I_n^1; \mathcal{H})}^2 + C_2 \tau_n^{\frac{2qp(k)}{\beta}} \left\| \frac{du^{n+1}(t)}{dt} \right\|_{L^2(I_n^1; V^{p(k)})}^2 \right. \\ &\quad \left. + C_3 \left\| \frac{du^{n+1}(t)}{dt} \right\|_{L^2(I_n^1; \mathcal{H})}^2 + C_4 \tau_n^{\frac{2(1-q)p(k)}{\gamma}} \left\| \frac{du^{n+1}(t)}{dt} \right\|_{L^2(I_n^1; V^{p(k)})}^2 \right], \end{aligned}$$

$$(3.27) \quad \begin{aligned} \text{NLT}_j &\leq C_L C_j^* \left[C_1 \left\| \frac{du^{n+1}(t)}{dt} \right\|_{L^2(I_n^1; \mathcal{H})}^2 + C_2 (\tau_n \tau_{n-j})^{\frac{qp(k)}{\beta}} \left\| \frac{du^{n+1}(t)}{dt} \right\|_{L^2(I_n^1; V^{p(k)})}^2 \right. \\ &\quad \left. + C_3 \left\| \frac{du^{n-j+1}(t)}{dt} \right\|_{L^2(I_{n-j}^1; \mathcal{H})}^2 + C_4 (\tau_n \tau_{n-j})^{\frac{(1-q)p(k)}{\gamma}} \left\| \frac{du^{n-j+1}(t)}{dt} \right\|_{L^2(I_{n-j}^1; V^{p(k)})}^2 \right]. \end{aligned}$$

We now pick q and $p(k)$ in the following manner

$$(3.28) \quad \begin{cases} q = \frac{1}{1 + \gamma/\beta}, & p(k) = \frac{(\beta + \gamma)k}{2}, & \text{if } \beta > 0, \gamma > 0, \\ q = 0, & p(k) = \frac{(\beta + \gamma)k}{2}, & \text{if } \beta = 0, \gamma > 0, \\ q = 1, & p(k) = \frac{(\beta + \gamma)k}{2}, & \text{if } \beta > 0, \gamma = 0. \end{cases}$$

We then have

$$(3.29) \quad \begin{cases} \frac{2qp(k)}{\beta} = k, & \frac{2(1-q)p(k)}{\gamma} = k, & \text{if } \beta > 0, \gamma > 0, \\ & \frac{2(1-q)p(k)}{\gamma} = k, & \text{if } \beta = 0, \gamma > 0, \\ & \frac{2qp(k)}{\beta} = k, & \text{if } \beta > 0, \gamma = 0. \end{cases}$$

Then estimates (3.26)–(3.27) give

$$(3.30) \quad \begin{aligned} \text{NLT}_0 \leq & C_L \left[C_1 \left\| \frac{du^{n+1}(t)}{dt} \right\|_{L^2(I_n^1; \mathcal{H})}^2 + C_2 \tau_n^k \left\| \frac{du^{n+1}(t)}{dt} \right\|_{L^2(I_n^1; V^{p(k)})}^2 \right. \\ & \left. + C_3 \left\| \frac{du^{n+1}(t)}{dt} \right\|_{L^2(I_n^1; \mathcal{H})}^2 + C_4 \tau_n^k \left\| \frac{du^{n+1}(t)}{dt} \right\|_{L^2(I_n^1; V^{p(k)})}^2 \right], \end{aligned}$$

$$(3.31) \quad \begin{aligned} \text{NLT}_j \leq & C_L C_j^* \left[C_1 \left\| \frac{du^{n+1}(t)}{dt} \right\|_{L^2(I_n^1; \mathcal{H})}^2 + C_2 (\tau_n \tau_{n-j})^{k/2} \left\| \frac{du^{n+1}(t)}{dt} \right\|_{L^2(I_n^1; V^{p(k)})}^2 \right. \\ & \left. + C_3 \left\| \frac{du^{n-j+1}(t)}{dt} \right\|_{L^2(I_{n-j}^1; \mathcal{H})}^2 + C_4 (\tau_n \tau_{n-j})^{k/2} \left\| \frac{du^{n-j+1}(t)}{dt} \right\|_{L^2(I_{n-j}^1; V^{p(k)})}^2 \right]. \end{aligned}$$

Simplifying the expression in (3.26)–(3.27) with the convention of $C_0^* = 1$ and combining (3.30)–(3.31) with (3.12), we have

$$\begin{aligned}
& \left\| \frac{du^{n+1}(t)}{dt} \right\|_{L^2(I_n^1; \mathcal{H})}^2 + A\tau^k \left\| \frac{du^{n+1}(t)}{dt} \right\|_{L^2(I_n^1; V^{p(k)})}^2 + E(u^{n+1}) - E(u^n) \\
& \leq C_L \left(C_3 + C_1 \sum_{j=0}^{k-1} C_j^* \right) \left\| \frac{du^{n+1}(t)}{dt} \right\|_{L^2(I_n^1; \mathcal{H})}^2 + C_L \left(C_4 \tau_n^k + C_2 \sum_{j=0}^{k-1} C_j^* (\tau_n \tau_{n-j})^{k/2} \right) \left\| \frac{du^{n+1}(t)}{dt} \right\|_{L^2(I_n^1; V^{p(k)})}^2 \\
& \quad + C_L C_3 \sum_{j=1}^{k-1} C_j^* \left\| \frac{du^{n-j+1}(t)}{dt} \right\|_{L^2(I_{n-j}^1; \mathcal{H})}^2 + C_L C_4 \sum_{j=1}^{k-1} C_j^* (\tau_n \tau_{n-j})^{k/2} \left\| \frac{du^{n-j+1}(t)}{dt} \right\|_{L^2(I_{n-j}^1; V^{p(k)})}^2 \\
& \leq C_L \left(C_3 + C_1 \sum_{j=0}^{k-1} C_j^* \right) \left\| \frac{du^{n+1}(t)}{dt} \right\|_{L^2(I_n^1; \mathcal{H})}^2 + C_L C_3 \sum_{j=1}^{k-1} C_j^* \left\| \frac{du^{n-j+1}(t)}{dt} \right\|_{L^2(I_{n-j}^1; \mathcal{H})}^2 \\
& \quad + C_L \left(C_4 \tau^k + C_2 \sum_{j=0}^{k-1} C_j^* \tau^k \right) \left\| \frac{du^{n+1}(t)}{dt} \right\|_{L^2(I_n^1; V^{p(k)})}^2 + C_L C_4 \sum_{j=1}^{k-1} C_j^* \tau^k \left\| \frac{du^{n-j+1}(t)}{dt} \right\|_{L^2(I_{n-j}^1; V^{p(k)})}^2 \\
& = C_L (C_3 + C_1 \overline{C}_0) \left\| \frac{du^{n+1}(t)}{dt} \right\|_{L^2(I_n^1; \mathcal{H})}^2 + C_L C_3 \sum_{j=1}^{k-1} C_j^* \left\| \frac{du^{n-j+1}(t)}{dt} \right\|_{L^2(I_{n-j}^1; \mathcal{H})}^2 \\
& \quad (3.32) \\
& \quad + C_L (C_4 + C_2 \overline{C}_0) \tau^k \left\| \frac{du^{n+1}(t)}{dt} \right\|_{L^2(I_n^1; V^{p(k)})}^2 + C_L C_4 \sum_{j=1}^{k-1} C_j^* \tau^k \left\| \frac{du^{n-j+1}(t)}{dt} \right\|_{L^2(I_{n-j}^1; V^{p(k)})}^2,
\end{aligned}$$

where the property of τ has been used.

Adding $C_L C_3 \sum_{j=1}^{k-2} \bar{C}_{j+1} \left\| \frac{du^{n-j+1}(t)}{dt} \right\|_{L^2(I_{n-j}^1; \mathcal{H})}^2$ and $C_L C_4 \sum_{j=1}^{k-2} \bar{C}_{j+1} \tau^k \left\| \frac{du^{n-j+1}(t)}{dt} \right\|_{L^2(I_{n-j}^1; V^{p(k)})}^2$ to both sides of (3.32), and utilizing (3.18), we deduce

$$\begin{aligned}
& E(u^{n+1}) + (1 - C_L (C_3 + C_1 \bar{C}_0)) \left\| \frac{du^{n+1}(t)}{dt} \right\|_{L^2(I_n^1; \mathcal{H})}^2 \\
& + (A - C_L (C_4 + C_2 \bar{C}_0)) \tau^k \left\| \frac{du^{n+1}(t)}{dt} \right\|_{L^2(I_n^1; V^{p(k)})}^2 \\
& + C_L C_3 \sum_{j=1}^{k-2} \bar{C}_{j+1} \left\| \frac{du^{n-j+1}(t)}{dt} \right\|_{L^2(I_{n-j}^1; \mathcal{H})}^2 + C_L C_4 \sum_{j=1}^{k-2} \bar{C}_{j+1} \tau^k \left\| \frac{du^{n-j+1}(t)}{dt} \right\|_{L^2(I_{n-j}^1; V^{p(k)})}^2 \\
& \leq E(u^n) + C_L C_3 \sum_{j=1}^{k-1} C_j^* \left\| \frac{du^{n-j+1}(t)}{dt} \right\|_{L^2(I_{n-j}^1; \mathcal{H})}^2 + C_L C_4 \sum_{j=1}^{k-1} C_j^* \tau^k \left\| \frac{du^{n-j+1}(t)}{dt} \right\|_{L^2(I_{n-j}^1; V^{p(k)})}^2 \\
& + C_L C_3 \sum_{j=1}^{k-2} \bar{C}_{j+1} \left\| \frac{du^{n-j+1}(t)}{dt} \right\|_{L^2(I_{n-j}^1; \mathcal{H})}^2 + C_L C_4 \sum_{j=1}^{k-2} \bar{C}_{j+1} \tau^k \left\| \frac{du^{n-j+1}(t)}{dt} \right\|_{L^2(I_{n-j}^1; V^{p(k)})}^2 \\
& = E(u^n) + C_L C_3 \bar{C}_1 \left\| \frac{du^n(t)}{dt} \right\|_{L^2(I_{n-1}^1; \mathcal{H})}^2 + C_L C_4 \bar{C}_1 \tau^k \left\| \frac{du^n(t)}{dt} \right\|_{L^2(I_{n-1}^1; V^{p(k)})}^2 \\
& (3.33) \\
& + C_L C_3 \sum_{j=2}^{k-1} \bar{C}_j \left\| \frac{du^{n-j+1}(t)}{dt} \right\|_{L^2(I_{n-j}^1; \mathcal{H})}^2 + C_L C_4 \sum_{j=2}^{k-1} \bar{C}_j \tau^k \left\| \frac{du^{n-j+1}(t)}{dt} \right\|_{L^2(I_{n-j}^1; V^{p(k)})}^2.
\end{aligned}$$

Then the modified energy decaying property (3.24) follows from (3.20)–(3.21) and (3.33). \square

Remark 3.6. For the case of $\beta = \gamma = 0$, the nonlinear terms in (3.13) can be bounded by $C_0 \tau_n \left\| \frac{du^{n+1}}{dt} \right\|_{L^2(I_n^1; \mathcal{H})}^2 + \sum_{j=1}^{k-1} \tau_n \left\| \frac{du^{n-j+1}}{dt} \right\|_{L^2(I_{n-j}^1; \mathcal{H})}^2$ where we have used the boundedness of step ratios of neighboring k -steps. Therefore, we can define a modified energy of the form of $\tilde{E}(u^n) = E(u^n) + \sum_{j=1}^{k-1} \tilde{C}_j \tau_n \left\| \frac{du^{n-j+1}(t)}{dt} \right\|_{L^2(I_{n-j}^1; \mathcal{H})}^2$ with $\tilde{C}_{j+1} r_c + 1 \leq \tilde{C}_j$ where r_c is a bound on neighboring k step sizes. Such non-negative choices of \tilde{C}_j s are always possible. We can demonstrate the monotonic decreasing property of the modified energy without the regularization term in the energy equality (3.12) provided that the time-step is small ($(C_0 + \tilde{C}_1 r_c) \tau_n \leq 1, \tau_n \leq \tilde{C}_{k-1}$). Thus no additional regularization term is required for energy stability, but a constant restriction for time step-size τ is needed.

4. CONVERGENCE ANALYSIS

In this section, we provide the optimal error estimate for the temporal discrete scheme (3.1) on any finite time interval $[0, T]$ assuming that the solution is sufficiently smooth so that assumption 3 is satisfied.

Let $u(t)$ the exact solution of (2.2) and define the error function $e(t) = u(t) - u^{n+1}(t)$, $e^j = e(t_j) = u(t_j) - u^j$, then the error equation becomes

$$\begin{aligned}
 & \frac{de(t)}{dt} + \epsilon \mathcal{L}e(t) + A\tau^k \frac{d}{dt} \mathcal{L}^{p(k)} e(t) \\
 &= A\tau^k \frac{d}{dt} \mathcal{L}^{p(k)} u(t) + F(u(t)) - \sum_{i=0}^{k-1} \ell_i(t - t_n) F(u^{n-i}) \\
 (4.1) \quad &:= R_1 + NL_1 + NL_2,
 \end{aligned}$$

where

$$\begin{aligned}
 R_1 &= A\tau^k \frac{d}{dt} \mathcal{L}^{p(k)} u(t), \\
 NL_1 &= F(u(t)) - \sum_{i=0}^{k-1} \ell_i(t - t_n) F(u(t_{n-i})), \\
 NL_2 &= \sum_{i=0}^{k-1} \ell_i(t - t_n) F(u(t_{n-i})) - \sum_{i=0}^{k-1} \ell_i(t - t_n) F(u^{n-i}).
 \end{aligned}$$

Assume

$$(4.2) \quad \lambda = 1 - \beta.$$

Taking the inner product of (4.1) with $\mathcal{L}^\lambda e(t)$ in \mathcal{H} , we have for some generic constant C ,

$$\begin{aligned}
 & \frac{1}{2} \frac{d}{dt} \|e(t)\|_{V^\lambda}^2 + \epsilon \|e(t)\|_{V^{\lambda+1}}^2 + \frac{1}{2} A\tau^k \frac{d}{dt} \|e(t)\|_{V^{p(k)+\lambda}}^2 \\
 &= \left(R_1 + NL_1 + NL_2, \mathcal{L}^\lambda e(t) \right)_{\mathcal{H}} \\
 (4.3) \quad & \leq C \|R_1\|_{V^{\lambda-1}}^2 + C \|NL_1\|_{V^{\lambda-1}}^2 + \frac{\epsilon}{4} \|e(t)\|_{V^{\lambda+1}}^2 + \left(NL_2, \mathcal{L}^\lambda e(t) \right)_{\mathcal{H}}.
 \end{aligned}$$

It is easy to see

$$(4.4) \quad \|R_1\|_{V^{\lambda-1}}^2 \leq C\tau^{2k} \left\| \frac{du}{dt} \right\|_{V^{2p(k)+\lambda-1}}^2.$$

For NL_1 , the properties of Lagrange interpolation give

$$\begin{aligned}
 NL_1 &= \sum_{i=0}^{k-1} \ell_i(t - t_n) [F(u(t)) - F(u(t_{n-i}))] \\
 (4.5) \quad &= \frac{1}{k!} \sum_{i=0}^{k-1} \ell_i(t - t_n) \int_t^{t_{n-i}} (t_{n-i} - t)^{k-1} (F(u(s)))_s^{(k)} ds,
 \end{aligned}$$

where $(F(u(s)))_s^{(k)}$ represents the k -th derivative with respect to s . Applying Hölder inequality to (4.5), we have

$$(4.6) \quad \|NL_1\|_{V^{\lambda-1}}^2 \leq C \tau^{2k-1} \|F(u(s))\|_{H^k(I_{n-k+1}^k; V^{\lambda-1})}^2.$$

Next, we turn to the other nonlinear term, NL_2 . By (2.4) one has

$$\begin{aligned}
 (NL_2, \mathcal{L}^\lambda e(t))_{\mathcal{H}} &= \sum_{i=0}^{k-1} \ell_i(t - t_n) (F(u(t_{n-i})) - F(u^{n-i}), \mathcal{L}^\lambda e(t))_{\mathcal{H}} \\
 &\leq \sum_{i=0}^{k-1} |\ell_i(t - t_n)| \|F(u(t_{n-i})) - F(u^{n-i})\|_{V^{-\beta}} \|e(t)\|_{V^{2\lambda+\beta}} \\
 &\leq C_L \sum_{i=0}^{k-1} |\ell_i(t - t_n)| \|e^{n-i}\|_{V^\gamma} \|e(t)\|_{V^{2\lambda+\beta}} \\
 (4.7) \quad &\leq \sum_{i=0}^{k-1} C C_L^2 \|e^{n-i}\|_{V^\gamma}^2 + \frac{\epsilon}{4} \|e(t)\|_{V^{2\lambda+\beta}}^2.
 \end{aligned}$$

Combining (4.3), (4.6) and (4.7), we obtain

$$\begin{aligned}
 &\frac{1}{2} \frac{d}{dt} \|e(t)\|_{V^\lambda}^2 + \frac{3\epsilon}{4} \|e(t)\|_{V^{\lambda+1}}^2 + \frac{1}{2} A \tau^k \frac{d}{dt} \|e(t)\|_{V^{p(k)+\lambda}}^2 \\
 &\leq C C_L^2 \sum_{i=0}^{k-1} \|e^{n-i}\|_{V^\gamma}^2 + \frac{\epsilon}{4} \|e(t)\|_{V^{2\lambda+\beta}}^2 \\
 (4.8) \quad &+ C \tau^{2k} \left\| \frac{du}{dt} \right\|_{V^{2p(k)+\lambda-1}}^2 + C \tau^{2k-1} \|F(u)\|_{H^k(I_{n-k+1}^k; V^{\lambda-1})}^2.
 \end{aligned}$$

Note that $\beta = 1 - \lambda$, then $2\lambda + \beta = \lambda + 1$. Denote $w(t) = \|e(t)\|_{V^\lambda}^2 + A \tau^k \|e(t)\|_{V^{p(k)+\lambda}}^2$, then (4.8) can be written as

$$\begin{aligned}
 (4.9) \quad &\frac{d}{dt} w(t) + \epsilon \|e(t)\|_{V^{\lambda+1}}^2 \leq C C_L^2 \sum_{i=0}^{k-1} \|e^{n-i}\|_{V^\gamma}^2 + C \tau^{2k} \left\| \frac{du}{dt} \right\|_{V^{2p(k)-\beta}}^2 + C \tau^{2k-1} \|F(u)\|_{H^k(I_{n-k+1}^k; V^{-\beta})}^2.
 \end{aligned}$$

Since $\gamma \leq 1 - \beta = \lambda$, we have $\|e^{n-i}\|_{V^\gamma}^2 \leq w^{n-i}$. Integrating (4.9) from t_n to t_{n+1} , we deduce

$$(4.10) \quad w(t_{n+1}) - w(t_n) \leq C C_L^2 \sum_{i=0}^{k-1} w^{n-i} \tau_n dt + C \tau^{2k} \left\| \frac{du}{dt} \right\|_{L^2(I_n^1, V^{2p(k)-\beta})}^2 + C \tau^{2k} \|F(u)\|_{H^k(I_{n-k+1}^k; V^{-\beta})}^2.$$

Summing up for n from $k-1$ to m , utilizing the assumptions on $\frac{du}{dt}$ and $F(u)$ with $t_{m+1} \leq T$, we have

$$(4.11) \quad w^{m+1} - w^{k-1} \leq C C_L^2 \sum_{n=k-1}^m \sum_{i=0}^{k-1} w^{n-i} \tau_n + C \tau^{2k}.$$

In order to apply the discrete Gronwall's inequality in summation form, we impose the following time-step ratio on neighboring k steps (**local time-step ratio**). More specifically, we assume there exists $r_c > 0$, such that

$$(4.12) \quad \frac{\tau_n}{\tau_m} \leq r_c, \quad \forall n, m, \text{ s.t. } |n - m| < k.$$

If we further assume that the initial errors are of the order of k , i.e., $w^j \leq C \tau^{2k}$, $j = 0, \dots, k-1$, we deduce from (4.11)

$$(4.13) \quad w^{m+1} \leq C C_L^2 \sum_{n=1}^m w^n \tau_{n-1} + C \tau^{2k}.$$

We have, thanks to discrete Gronwall inequality

$$(4.14) \quad w^m \leq C \tau^{2k}, \quad \forall t_m \in [0, T].$$

Therefore, we have proved the following optimal error estimates

Theorem 4.1. *For $\lambda = 1 - \beta$. Assume $F(u) \in H^k(0, T; V^{-\beta})$ and $u \in H^1(0, T; V^{2p(k)-\beta})$, $\|e^j\|_{V^\lambda}^2 + A \tau^k \|e^j\|_{V^{p(k)+\lambda}}^2 \leq C \tau^{2k}$, $j = 0, 1, \dots, k-1$; $\beta + \gamma \leq 1$, $\tau < 1$, and the local time-step ratio is bounded by a constant r independent of the time step τ_n , i.e., (4.12) is valid. Then the scheme converges with the optimal rate of k in the sense that*

$$(4.15) \quad \|e^n\|_{V^\lambda}^2 + A \tau^k \|e^n\|_{V^{p(k)+\lambda}}^2 \leq C \tau^{2k}, \quad \forall n \text{ s.t. } t_n \leq T.$$

5. APPLICATION TO NO-SLOPE-SELECTION (NSS) THIN-FILM EPITAXIAL GROWTH MODEL

In this section, we show that the abstract framework applies to the no-slope-selection (NSS) thin-film epitaxial growth equation:

$$(5.1) \quad \frac{\partial u}{\partial t} = -\epsilon \Delta^2 u - \nabla \cdot \left(\frac{\nabla u}{1 + |\nabla u|^2} \right)$$

with periodic boundary condition imposed. The energy functional is given by

$$(5.2) \quad E(u) = \int_{\Omega} \left(\frac{\epsilon}{2} |\Delta u|^2 - \frac{1}{2} \ln(1 + |\nabla u|^2) \right) d\mathbf{x}.$$

The linear and nonlinear operators are $\mathcal{L} = \Delta^2$ and $F(u) = -\nabla \cdot \left(\frac{\nabla u}{1 + |\nabla u|^2} \right)$, respectively. Therefore, the abstract functional spaces are specified to $\mathcal{H} = \{f : f \in L^2 \text{ with zero mean}\}$, $V^{\frac{1}{2}} = \{f : f \in H_{per}^2 \text{ with zero mean}\}$.

In the following, we will verify the assumptions proposed in Section 2 for the NSS equation one by one. First we note that the norm equivalence between $\|v\|_{H^2}$ and $\|\Delta v\|$ follows from the elliptic regularity and Poincaré's inequality. Secondly, the Lipschitz continuity (2.4) with $\beta = \gamma = \frac{1}{2}$, $C_L = 1$ has been verified in [9], i.e.,

$$(5.3) \quad \|F(u) - F(v)\|_{V^{-\frac{1}{2}}} \leq \|u - v\|_{V^{\frac{1}{2}}}.$$

By (3.28), it yields $p(k) = k/2$. Therefore, the modified energy stability (3.24) establishes with

$$\begin{aligned} \tilde{E}_N(u^n) &= \left(-\frac{1}{2} \ln(1 + |\nabla u^n|^2), 1 \right)_{L^2} + \frac{\epsilon}{2} \|\Delta u^n\|_{L^2}^2 + C_L C_3 \sum_{j=1}^{k-1} \overline{C}_j \left\| \frac{du^{n-j+1}(t)}{dt} \right\|_{L^2(I_{n-j}^1; L^2)}^2 \\ &\quad + C_L C_4 \sum_{j=1}^{k-1} \overline{C}_j \tau^k \left\| \frac{d\Delta^{k/2} u^{n-j+1}(t)}{dt} \right\|_{L^2(I_{n-j}^1; L^2)}^2. \end{aligned}$$

Constructing proper initial step (the first $k-1$ steps) similar to that in [5] for solving (5.1), then we can obtain an upper bound for $\tilde{E}(u^n)$, from which the H^2 bound of numerical solution to (3.1) can be obtained (see [3]). Moreover, the H^3 bound for the numerical solution can be provided as long as the initial data is smooth enough (see [4, 5]). As for the boundedness (2.5), now $\lambda = 1 - \beta = \frac{1}{2}$ and

$$(5.4) \quad \|F(u)\|_{H^k(0,T;H^1)}^2 = \left\| -\nabla \cdot \left(\frac{\nabla u}{1 + |\nabla u|^2} \right) \right\|_{H^k(0,T;H^1)}^2 \leq C \|u\|_{W^{k,\infty}(0,T;H^3)}^2.$$

thus this boundedness can be guaranteed by requiring exact solution u to be smooth enough, say $u \in W^{k,\infty}(0,T;H^{m+2})$.

6. NUMERICAL RESULTS

In this section, we report numerical results when the variable-step second-order ETD-MS scheme on the NSS equation. More specifically, the scheme takes the following form

$$(6.1) \quad \begin{aligned} &\frac{du^{n+1}(t)}{dt} + \epsilon \Delta^2 u^{n+1}(t) + A \tau^2 \frac{d}{dt} \Delta^2 u^{n+1}(t) = -\nabla \cdot \left(\frac{\nabla u^n}{1 + |\nabla u^n|^2} \right) \\ &+ \frac{t - t_n}{\tau_n} \left(-\nabla \cdot \left(\frac{\nabla u^n}{1 + |\nabla u^n|^2} \right) + \nabla \cdot \left(\frac{\nabla u^{n-1}}{1 + |\nabla u^{n-1}|^2} \right) \right), \quad t \in [t_n, t_{n+1}]. \end{aligned}$$

N_T	L^2 error	convergence rate	L^2 error	convergence rate
1	5.258e-2	-	7.873e-2	-
2	1.658e-2	1.665	2.801e-2	1.4909
4	4.432e-3	1.903	7.807e-3	1.843
8	1.128e-3	1.973	2.011e-3	1.957
16	2.837e-4	1.992	5.071e-4	1.988
32	7.103e-5	1.998	1.271e-4	1.996
64	1.777e-5	1.999	3.181e-5	1.999

TABLE 1. L^2 errors on uniform initial time grid(the second column) and random initial time mesh(the fourth column), the time step $\Delta t = \Delta t_0/N_T$ for the uniform time grid.

Both the temporal convergence and long-time energy stability are validated. The two dimensional domain $\Omega = [0, 2\pi]^2$ with periodic boundary condition is considered and the Fourier pseudo-spectral method is applied for spatial discretization.

6.1. Temporal convergence. In this subsection, the second-order temporal convergence is tested at the terminal time $T = 1$. The parameters are set as $L = 4\pi$, $\epsilon = 0.01$. The construction of variable time steps is completed via a uniform time grid plus 10% random perturbation; the specific implementation is referred to [50, Section 6.1, p.518]. More specifically, the coarsest grid is obtained by setting a uniform partition with step-size $\Delta t_0 = 0.0025$, and then adding a 10% random perturbation onto time grids to make new variable-step time-step series. The finer one is to double the number of time nodes with the nodes set as $t_k^{fine} = t_{(k+1)/2}^{coarse}$ for odd k , and $t_k^{fine} = (t_{k-1}^{fine} + t_{k+1}^{fine})/2$ for even k .

Simple calculation shows $C_0^* = 1$, $C_1^* = 1/\sqrt{3}$ and $\overline{C}_0 = 1 + 1/\sqrt{3}$. The constants in (3.4) are $C_1 = \frac{1}{4}\hat{C}^2$, $C_2 = \frac{1}{4}\hat{C}^{-2}$, $C_3 = \frac{1}{4}\tilde{C}^2$, $C_4 = \frac{1}{4}\tilde{C}^{-2}$. Then we can take $\hat{C}^2 = \tilde{C}^2 = \frac{6}{3+\sqrt{3}}$ and $A = \left(\frac{3+\sqrt{3}}{6}\right)^2 = \frac{2+\sqrt{3}}{6}$.

To compute the error, an artificial forcing term is added so that the exact solution is given by $u(t) = \cos(t) \sin(x) \cos(y)$. Table 1 exhibits the L^2 error, in which the second-order accuracy is validated. And we can find that the errors on the uniform time mesh are smaller than those on the nonuniform mesh.

6.2. Coarsening process. In this subsection, we simulate the physically interesting coarsening process. The parameters are $L = 4\pi$, $\epsilon = 0.005$, $T = 40000$. The variable-step time nodes are made upon a uniform grid $\Delta t = 0.001$ plus 10% random perturbation. Some relevant physical quantities, the energy E , the average height h and the average slope m

are defined by

$$E(u) = \left(-\frac{1}{2} \ln(1 + |\nabla u|^2), 1 \right) + \frac{\varepsilon}{2} \|\Delta u\|^2,$$

$$h(u, t) = \sqrt{\frac{h^2}{|\Omega|} \sum_x |u(x, t) - \bar{u}(t)|^2}, \quad \text{with} \quad \bar{u}(t) := \frac{h^2}{|\Omega|} \sum_x u(x, t),$$

$$m(u, t) = \sqrt{\frac{h^2}{|\Omega|} \sum_x |\nabla u(\mathbf{x}_{i,j}, t)|^2},$$

and it has been proved $E \sim O(-\ln(t))$, $h \sim O(t^{\frac{1}{2}})$ and $m \sim O(t^{\frac{1}{4}})$ as $t \rightarrow \infty$ (see [24, 36, 37]). The snapshots of numerical solution at time $t = 0.99997, 5000, 15000, 20000, 30000, 40000$ are shown in Figure 1. The scaling laws of energy E , average height h and average slope m are verified in Figures 2–3.

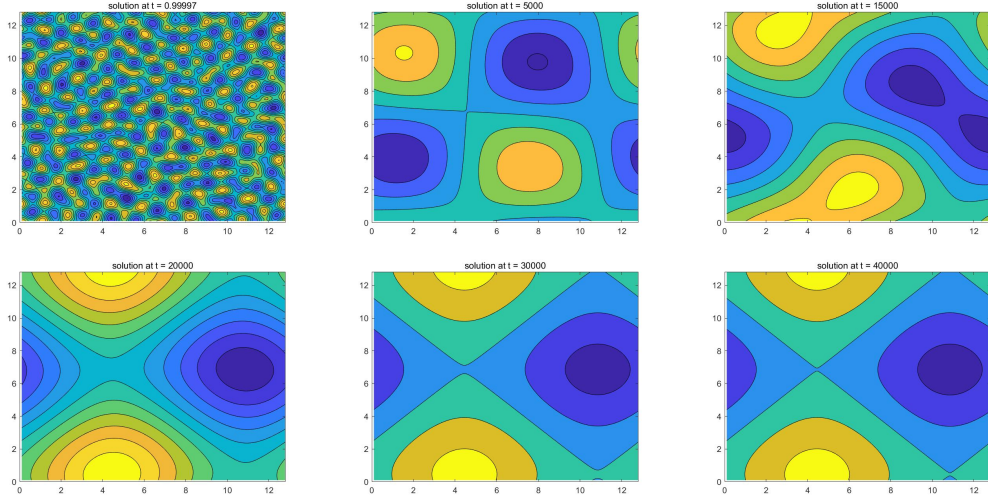


FIGURE 1. Snapshots of the numerical solutions for scheme (6.1).

6.3. Adaptive results. The solutions of phase field models can exhibit rapid variations over short time intervals, while remaining relatively steady over others. One key benefit of unconditionally energy stable schemes is their natural compatibility with adaptive time-stepping algorithms, where the time step is determined solely by accuracy requirements rather than stability constraints. In contrast, many other numerical schemes face significant challenges when combined with adaptive time stepping, as they often lack robust stability under variable time steps. This highlights the importance of high-order unconditionally energy stable variable step methods.

For gradient flows, there are several effective adaptive time stepping strategies, see [66–68]. Here we use the strategy summarized in the following Algorithm, where the time step

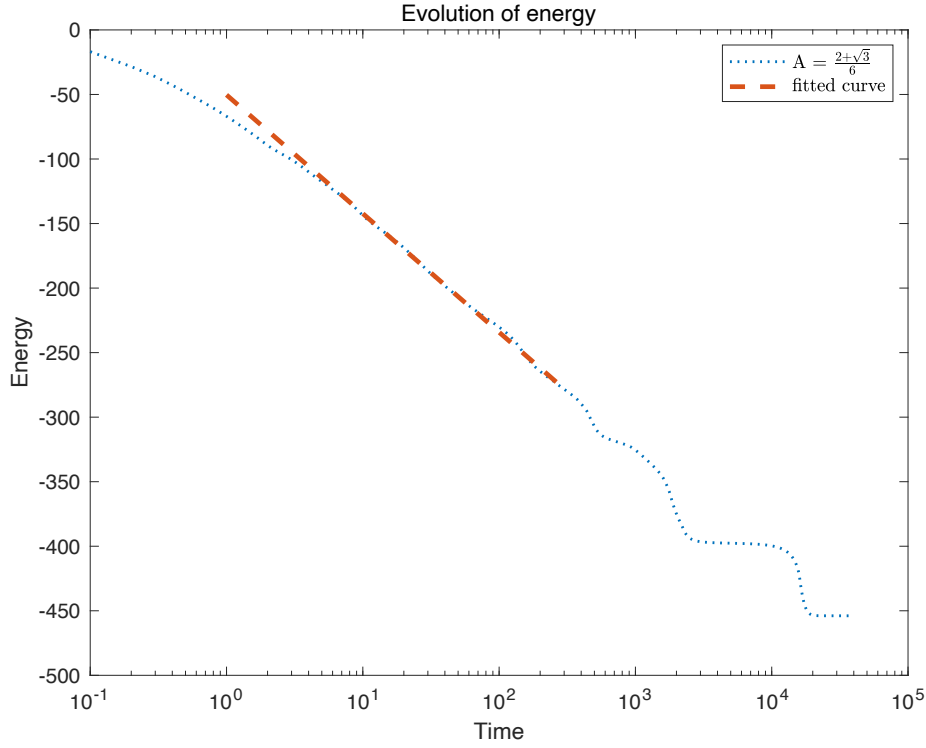


FIGURE 2. Semi-log plot of the energy E . Fitted line has the form $a \ln(t)+b$, with coefficients $a = -39.93$, $b = -50.33$.

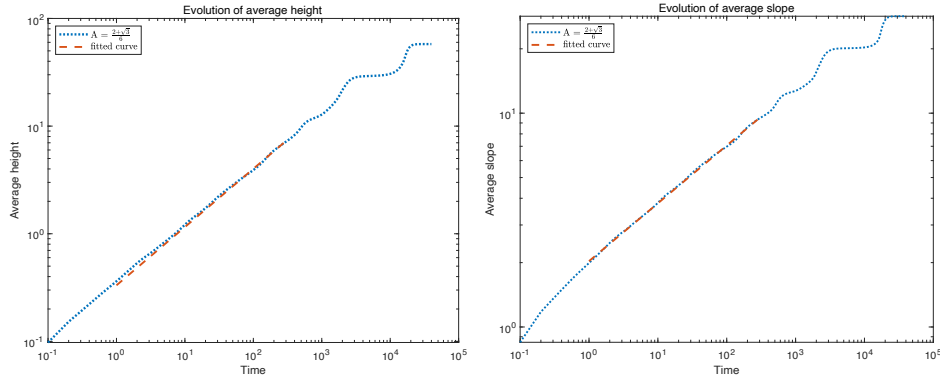


FIGURE 3. The log-log plot of (1) the average surface height h and (2) the average slope m . Fitted lines have the form at^b , with coefficients (1) $a = 0.3319$, $b = 0.5414$ and (2) $a = 2.032$, $b = 0.2705$.

is updated by the formula

$$(6.2) \quad A_{dp}(e, \tau) = \rho \left(\frac{tol}{e} \right)^r \tau,$$

along with the restriction of the minimum and maximum time steps. In the above formula, ρ is a default safety coefficient, tol is a reference tolerance, e is the relative error computed at each time level in Step 3, and r is the adaptive rate. In our numerical examples, we set $\rho = 0.95$ and $tol = 10^{-3}$, the minimum time step is 10^{-3} , while the maximum time step is $\tau = 10^{-1}$ for Figure 4. The initial condition is given by $u = \sin(x) \cos(y) + 0.5 * (2 * \text{rand} - 1)$ where rand represents a uniformly distributed random noise in $[0, 1]$, and the initial time step is taken as the minimum time step.

Algorithm 1 Adaptive time stepping procedure

Given: U^n, τ_n

Step 1. Compute U_1^{n+1} by the first-order ETD scheme with τ_n .

Step 2. Compute U_2^{n+1} by the second-order ETDMS scheme (6.1) with τ_n .

Step 3. Calculate $e_{n+1} = \frac{\|U_1^{n+1} - U_2^{n+1}\|}{\|U_2^{n+1}\|}$.

Step 4. If $e_{n+1} > tol$, recalculate the time step

$$\tau_n \leftarrow \max\{\tau_{min}, \min\{A_{dp}(e_{n+1}, \tau_n), \tau_{max}\}\},$$

Step 5. goto Step 1.

Step 6. else, update the time step $\tau_{n+1} \leftarrow \max\{\tau_{min}, \min\{A_{dp}(e_{n+1}, \tau_n), \tau_{max}\}\}$.

Step 7. endif

We take $\epsilon = 0.005$, $N = 128$ and as a comparison, the first and third rows in Figure 4 exhibit snapshots of the numerical result generated by the second-order ETDMS solutions with uniform time step size $\tau = 10^{-1}$ and $\tau = 10^{-3}$, respectively, while the second row displays snapshots generated by the adoptive scheme starting from the same initial data. The last row presents the magnitudes of time steps and the energy evolution. We observe that the solution using large time step (first row) even cannot get the correct topological changes. We also observe from the last row that the adaptive time steps basically stay around the maximum size at large time, indicating that the computational cost is almost the same as the large-step solution. In addition, we can also observe that the energy curve has a similar evolution as in Figure 2. This experiment proves that with the unconditionally energy-stable ETDMS schemes, the adaptive algorithm only takes as little computational cost as that of large time steps, while achieving the same level of accuracy as small time steps.

7. CONCLUSION

Extending our recent work [6], a generic variable-step k^{th} -order linear scheme was proposed for gradient flows by using ETD-MS method. Under the assumption that the non-linearity is Lipschitz continuous in some appropriate sense, we have demonstrated that the scheme is long time stable in the sense that a modified energy is a monotonic function of the

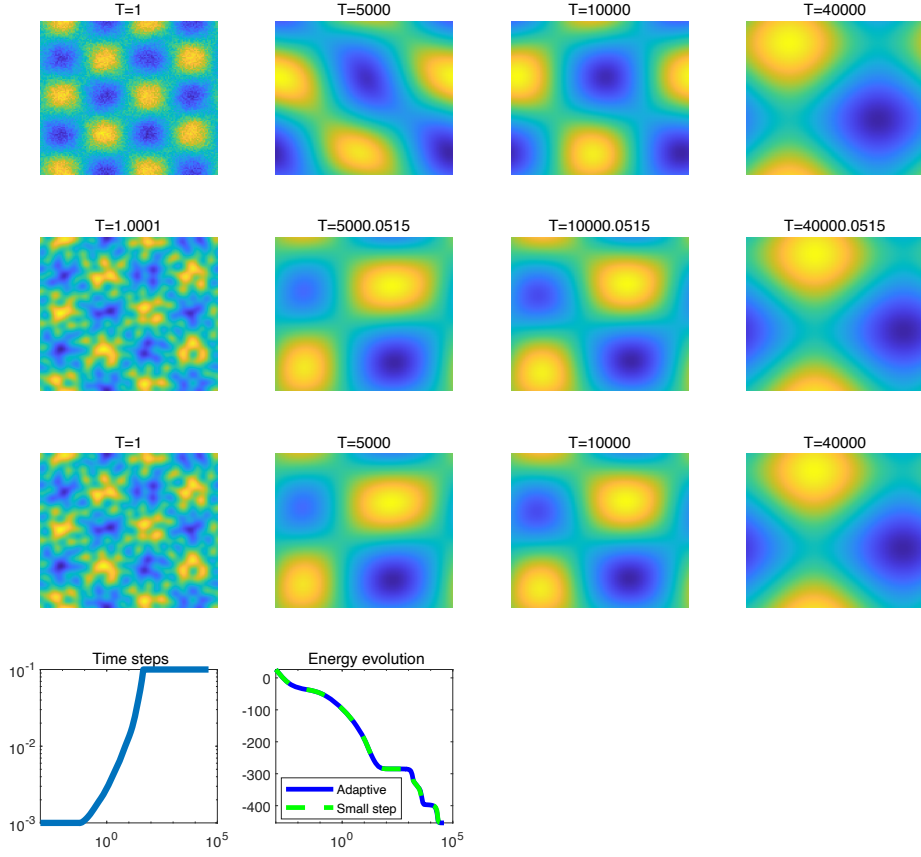


FIGURE 4. Solutions using large time steps $\tau = 0.1$ (first line), adaptive time steps (second line) and small time steps $\tau = 0.001$ (third line), and time steps curve and energy evolution (fourth line)

time. In addition, we proved the k^{th} -order accuracy in the $\ell^\infty(0, T; V^\lambda)$ norm assuming a maximal time step-size 1 and a bound on local (neighboring- k) time-step ratio. Numerical experiments on the thin film epitaxial growth without slope selection model confirm the stability and optimal rate of convergence. Using local error as an adaptive strategy, we also demonstrate the potential of the scheme as an efficient adaptive-in-time algorithm.

ACKNOWLEDGEMENTS

This work is supported in part by the grants NSFC 12241101, NSFC 12471369 (W. Chen), NSFC 11871159, NSFC 12271237 (X.Wang).

REFERENCES

- [1] Adams, R.A. and Fournier J.J.F.: Sobolev spaces. Academic press, Singapore (2003)
- [2] C. Canuto and A. Quarteroni: Approximation results for orthogonal polynomials in Sobolev spaces. *Math. Comp.* 38: 67–86, 1982
- [3] W. Chen, C. Wang, X. Wang, and S.M. Wise: A linear iteration algorithm for a second-order energy stable scheme for a thin film model without slope selection. *J. Sci. Comput.* 59: 574–601, 2014
- [4] W. Chen, W. Li, Z. Luo, C. Wang, and X. Wang: A stabilized second order exponential time differencing multistep method for thin film growth model without slope selection. *ESAIM: Math. Model. Numer. Anal.*, 54(3): 727–750, 2020.
- [5] W. Chen, W. Li, C. Wang, S. Wang, and X. Wang: Energy stable higher-order linear ETD multi-step methods for gradient flows: application to thin film epitaxy. *Res. Math. Sci.*, 7(3): 1–27, 2020.
- [6] W. Chen, S. Wang, and X. Wang: Long-time stable arbitrary order ETD-MS method for gradient flows with Lipschitz nonlinearity. *CSIAM Trans. Appl. Math.*, Vol.2, Issue 3, 460–483, 2021.
- [7] W. Cao, H. Yang, and W. Chen: An exponential time differencing Runge-Kutta method ETDRK32 for phase field models. *J. Sci. Comput.* 99, 6(2024).
- [8] H. Yang, W. Cao, W. Chen: Energy Stability of Adaptive Exponential Time Difference Runge-Kutta Method (ETDRK32). *J. Sci. Comput.* 103, 28 (2025).
- [9] L. Ju, X. Li, Z. Qiao, and H. Zhang: Energy stability and error estimates of exponential time differencing schemes for the epitaxial growth model without slope selection. *Math. Comp.* 87, 1859–1885, 2017.
- [10] S. M. Allen and J. W. Cahn: A microscopic theory for antiphase boundary motion and its application to antiphase domain coarsening. *Acta Metall.*, 27(6):1085–1095, 1979.
- [11] L. Ambrosio, N. Gigli, and G. Savaré: Gradient Flows in metric spaces and in the space of probability measures, 2nd ed. Birkhauser, 2008.
- [12] D. M. Anderson, G. B. McFadden, and A. A. Wheeler: Diffuse-interface methods in fluid mechanics. *Annu. Rev. Fluid Mech.*, 30(1): 139–165, 1998.
- [13] G. Beylkin, J. M. Keiser and L. Vozovoi: A new class of time discretization schemes for the solution of nonlinear PDEs. *J. Comput. Phys.*, 147(2): 362–387, 1998.
- [14] L. A. Caffarelli and N. E. Muler: An L^∞ bound for solutions of the Cahn-Hilliard equation. *ArRMA*, 133(2): 129–144, 1995.
- [15] J. W. Cahn and J. E. Hilliard: Free energy of a nonuniform system. i. interfacial free energy. *J. Chem. Phys.*, 28(2): 258–267, 1958.
- [16] K. Cheng, Z. Qiao, and C. Wang: A third order exponential time differencing numerical scheme for no-slope-selection epitaxial thin film model with energy stability. *J. Sci. Comput.*, 81(1): 154–185, 2019.
- [17] S. M. Cox and P. C. Matthews. Exponential time differencing for stiff systems. *J. Comput. Phys.*, 176(2): 430–455, 2002.
- [18] M. Doi and S. F. Edwards: *The theory of polymer dynamics*, volume 73. Oxford University Press, 1988.
- [19] Q. Du and W. Zhu: Stability analysis and application of the exponential time differencing schemes. *J. Comput. Math.*, 200–209, 2004.
- [20] Q. Du and W. Zhu: Analysis and applications of the exponential time differencing schemes and their contour integration modifications. *BIT Numer. Math.*, 45(2): 307–328, 2005.
- [21] K. Elder, M. Katakowski, M. Haataja, and M. Grant: Modeling elasticity in crystal growth. *Phys. Rev. Lett.*, 88(24): 245701, 2002.
- [22] C. M. Elliott and A. Stuart: The global dynamics of discrete semilinear parabolic equations. *SIAM J. Numer. Anal.*, 30(6): 1622–1663, 1993.
- [23] D. J. Eyre: Unconditionally gradient stable time marching the Cahn-Hilliard equation. In *Mater. Res. Soc. Symp. Proc.*, 529: 39–46, 1998.
- [24] L. Golubovic: Interfacial coarsening in epitaxial growth models without slope selection. *Phys. Rev. Lett.*, 78(1): 90–93, 1997.

- [25] Y. Gong, J. Zhao, and Q. Wang: Arbitrarily high-order unconditionally energy stable sav schemes for gradient flow models. *Comput. Phys. Commun.*, 249:107033, 2020.
- [26] M. E. Gurtin, D. Polignone, and J. Vinals: Two-phase binary fluids and immiscible fluids described by an order parameter. *Math. Models Methods Appl. Sci.*, 6(06): 815–831, 1996.
- [27] E. Hairer, S. P. Noersett and G. Wanner: Solving ordinary differential equations i. nonstiff problems. *Springer Ser. Comput. Math.*, 8, 1993.
- [28] M. Hochbruck and A. Ostermann: Explicit exponential Runge–Kutta methods for semilinear parabolic problems. *SIAM J. Numer. Anal.*, 43(3): 1069–1090, 2005.
- [29] M. Hochbruck and A. Ostermann: Exponential integrators. *Acta Numer.*, 19(May): 209–286, 2010.
- [30] M. Hochbruck and A. Ostermann: Exponential multistep methods of Adams-type. *BIT Numer. Math.*, 51(4): 889–908, 2011.
- [31] L. Ju, X. Li, Z. Qiao, and H. Zhang: Energy stability and error estimates of exponential time differencing schemes for the epitaxial growth model without slope selection. *Math. Comp.*, 87(312): 1859–1885, 2018.
- [32] A. Kassam and L. N. Trefethen: Fourth-order time-stepping for stiff PDEs. *SIAM J. Sci. Comput.*, 26(4): 1214–1233, 2005.
- [33] R. V. Kohn and X. Yan: Upper bound on the coarsening rate for an epitaxial growth model. *Commun. Pure Appl. Math.*, 56(11): 1549–1564, 2003.
- [34] P. D. Lax: Functional Analysis. Wiley-Interscience, New York, 2002.
- [35] F. M. Leslie: Theory of flow phenomena in liquid crystals. *Adv. Liq. Cryst.*, 4:1–81, 1979.
- [36] B. Li and J. Liu: Thin film epitaxy with or without slope selection. *Euro. J. Appl. Math.*, 14(6): 713–743, 2003.
- [37] B. Li and J. Liu: Epitaxial growth without slope selection: Energetics, coarsening, and dynamic scaling. *J. Nonlinear Sci.*, 14(5): 429–451, 2004.
- [38] D. Moldovan and L. Golubovic: Interfacial coarsening dynamics in epitaxial growth with slope selection. *Phys. Rev. E*, 61(6): 6190, 2000.
- [39] Y. Morita and K. Tachibana: An entire solution to the Lotka–Volterra competition-diffusion equations. *SIAM J. Math. Anal.*, 40(6): 2217–2240, 2009.
- [40] C. Quan, X. Wang, P. Zheng, and Z. Zhou, Maximum bound principle and original energy dissipation of arbitrarily high-order ETD Runge-Kutta schemes for Allen-Cahn equations. *IMA Journal of Numerical Analysis*. accepted 2025. *arXiv:2404.19188*
- [41] J. Shen, C. Wang, X. Wang, and S. M. Wise: Second-order convex splitting schemes for gradient flows with Ehrlich–Schwoebel type energy: application to thin film epitaxy. *SIAM J. Numer. Anal.*, 50(1): 105–125, 2012.
- [42] J. Shen, J. Xu, and J. Yang: The scalar auxiliary variable (SAV) approach for gradient flows. *J. Comput. Phys.*, 353: 407–416, 2018.
- [43] J. Shen, J. Xu, and J. Yang: A new class of efficient and robust energy stable schemes for gradient flows. *SIAM Rev.*, 61(3): 474–506, 2019.
- [44] J. Shen and X. Yang: Numerical approximations of Allen-Cahn and Cahn-Hilliard equations. *Discrete Contin. Dyn. Syst. - A*, 28(4): 1669, 2010.
- [45] J. Shin, H. G. Lee, and J. Y. Lee: Unconditionally stable methods for gradient flow using convex splitting Runge–Kutta scheme. *J. Comput. Phys.*, 347: 367–381, 2017.
- [46] Y. Takeuchi: *Global dynamical properties of Lotka-Volterra systems*. World Scientific, 1996.
- [47] R. Temam: *Infinite-dimensional dynamical systems in mechanics and physics*, volume 68. Springer Science & Business Media, 1997.
- [48] C. Wang, X. Wang, and S. M. Wise: Unconditionally stable schemes for equations of thin film epitaxy. *Discrete Contin. Dyn. Syst. - A*, 28(1): 405, 2010.
- [49] P. Yue, J. J. Feng, C. Liu, and J. Shen: A diffuse-interface method for simulating two-phase flows of complex fluids. *J. Fluid Mech.*, 515:293, 2004.

- [50] W. Chen, X. Wang, Y. Yan, and Z. Zhang: A Second Order BDF Numerical Scheme with Variable Steps for the Cahn–Hilliard Equation. *SIAM J. Numer. Anal.*, 57(1), 495–525, 2019
- [51] A. Miranville: *The Cahn–Hilliard Equation: Recent Advances and Applications*, Society for Industrial and Applied Mathematics, 2019.
- [52] H. L. Liao, X. Song, T. Tang, and T. Zhou: Analysis of the second order BDF scheme with variable steps for the molecular beam epitaxial model without slope selection. *Sci. China Mathematics*, vol. 64, pp. 887–902, (2021).
- [53] W. Chen, Y. Zhang, W. Li, Y. Wang, and Y. Yan: Optimal convergence analysis of a second order scheme for a thin film model without slope selection. *J. Sci. Comput.*, 80(3): 1716–1730, 2019.
- [54] H. Liao, B. Ji, and L. Zhang: An adaptive BDF2 implicit time-stepping method for the phase field crystal model. *IMA Journal of Numerical Analysis*, Volume 42, Issue 1, January 2022, Pages 649–679, <https://doi.org/10.1093/imanum/draa075>.
- [55] W. Wang, M. Mao, and Z. Wang: Stability and error estimates for the variable step-size BDF2 method for linear and semilinear parabolic equations. *Advances in Computational Mathematics*, vol. 47, article no. 8, (2021).
- [56] Y. Hao, Q. Huang. and C. Wang: A third order BDF energy stable linear scheme for the no-slope-selection thin film model. *Commun. Comput. Phys.* 29(3): 905–929, 2020
- [57] R. Liang, Y. Yan, W. Chen. and Y. Wang: Super-Closeness between the Ritz Projection and the Finite Element Solution for some Elliptic Problems. *Commun. Comput. Phys.*, 28(2): 803–826, 2020.
- [58] H. L. Liao and Z. Zhang: Analysis of adaptive BDF2 scheme for diffusion equations. *Math. Comp.*, 90 (2021), 1207–1226. DOI: <https://doi.org/10.1090/mcom/3585>
- [59] H. L. Liao, T. Tang, and T. Zhou: On energy stable, maximum-principle preserving, second order BDF scheme with variable steps for the Allen-Cahn equation. *SIAM Journal on Numerical Analysis*, Vol. 58, Iss. 4 (2020)10.1137/19M1289157.
- [60] F. Huang, J. Shen, and Z. Yang: A highly efficient and accurate new SAV approach for gradient flows. *SIAM J. Sci. Comput.*, 42(4): A2514–A2536, 2020.
- [61] V. DeCaria and M. Schneier: An embedded variable step IMEX scheme for the incompressible Navier-Stokes equations. *Computer Methods in Applied Mechanics and Engineering*, Volume 376, 2021, 113661, ISSN 0045-7825, <https://doi.org/10.1016/j.cma.2020.113661>.
- [62] S. Wang, W. Chen, H. Pan, and C. Wang: Optimal rate convergence analysis of a second order scheme for a thin film model with slope selection. *J. Comput. Appl. Math.*, 377, 112855. 2020.
- [63] W. Cao, H. Yang, and W. Chen: An Exponential Time Differencing Runge–Kutta Method ETDRK32 for Phase Field Models. *J. Sci. Comput.*, 99(6), 2024.
- [64] Z. Fu and J. Yang: Energy-decreasing exponential time differencing Runge-Kutta methods for phase-field models. *J. Comput. Phys.*, 454(1): 110943, 2022.
- [65] Z. Fu, J. Shen, and J. Yang: Higher-order energy-decreasing exponential time differencing Runge-Kutta methods for gradient flows. *Sci. China Math.*, 68: 1727–1746, 2025.
- [66] W. Chen, M. Wang, Y. Yan, and Z. Zhang: A Second Order BDF Numerical Scheme with Variable Steps for the Cahn–Hilliard Equation. *SIAM J. Numer. Anal.*, 57(1): 495–525, 2019.
- [67] Y. He, Y. Liu, and T. Tang: On large time-stepping methods for the Cahn–Hilliard equation. *Appl. Numer. Math.*, 57: 616–628, 2006.
- [68] Z. Zhang and Z. Qiao: An Adaptive Time-Stepping Strategy for the Cahn–Hilliard Equation. *Commun. Comput. Phys.*, 11: 1261–1278, 2012.

(Wenbin Chen) SHANGHAI KEY LABORATORY FOR CONTEMPORARY APPLIED MATHEMATICS, SCHOOL OF MATHEMATICAL SCIENCES, FUDAN UNIVERSITY, SHANGHAI, CHINA 200433

Email address: `wbchen@fudan.edu.cn`

(Zhaohui Fu) DEPARTMENT OF MATHEMATICS, NATIONAL UNIVERSITY OF SINGAPORE, SINGAPORE, 119076

Email address: `fuzhmath@nus.edu.sg`

(Shufen Wang) SHENWAN HONGYUAN SECURITIES CO., LTD., SHANGHAI, CHINA 200031

Email address: `17110180015@fudan.edu.cn`

(Xiaoming Wang) SCHOOL OF MATHEMATICS SCIENCES, EASTERN INSTITUTE OF TECHNOLOGY, NINGBO, CHINA 315200

Email address: `wxm.math@outlook.com`